arXiv:hep-ex/0503039v3 14 Jun 2005

Search for Higgs Bosons Decaying into $b\bar{b}$ and Produced in Association with a Vector Boson in $p\bar{p}$ Collisions at $\sqrt{s} = 1.8$ TeV

D. Acosta,[1] T. Affolder,[2] M.G. Albrow,[3] D. Ambrose,[4] D. Amidei,[5] K. Anikeev,[6] J. Antos,[7] G. Apollinari,[3] T. Arisawa,[8] A. Artikov,[9] W. Ashmanskas,[10] F. Azfar,[11] P. Azzi-Bacchetta,[12] N. Bacchetta,[12] H. Bachacou,[13] W. Badgett,[3] A. Barbaro-Galtieri,[13] V.E. Barnes,[14] B.A. Barnett,[15] S. Baroiant,[16] M. Barone,[17] G. Bauer,[6] F. Bedeschi,[18] S. Behari,[15] S. Belforte,[19] W.H. Bell,[20] G. Bellettini,[18] J. Bellinger,[21] D. Benjamin,[22] A. Beretvas,[3] A. Bhatti,[23] M. Binkley,[3] D. Bisello,[12] M. Bishai,[3] R.E. Blair,[10] C. Blocker,[24] K. Bloom,[5] B. Blumenfeld,[15] A. Bocci,[23] A. Bodek,[25] G. Bolla,[14] A. Bolshov,[6] D. Bortoletto,[14] J. Boudreau,[26] C. Bromberg,[27] E. Brubaker,[13] J. Budagov,[9] H.S. Budd,[25] K. Burkett,[3] G. Busetto,[12] K.L. Byrum,[10] S. Cabrera,[22] M. Campbell,[5] W. Carithers,[13] D. Carlsmith,[21] A. Castro,[28] D. Cauz,[19] A. Cerri,[13] L. Cerrito,[29] J. Chapman,[5] C. Chen,[4] Y.C. Chen,[7] M. Chertok,[16] G. Chiarelli,[18] G. Chlachidze,[3] F. Chlebana,[3] M.L. Chu,[7] J.Y. Chung,[30] W.-H. Chung,[21] Y.S. Chung,[25] C.I. Ciobanu,[29] A.G. Clark,[31] M. Coca,[25] A. Connolly,[13] M. Convery,[23] J. Conway,[32] M. Cordelli,[17] J. Cranshaw,[33] R. Culbertson,[3] D. Dagenhart,[24] S. D'Auria,[20] P. de Barbaro,[25] S. De Cecco,[34] S. Dell'Agnello,[17] M. Dell'Orso,[18] S. Demers,[25] L. Demortier,[23] M. Deninno,[28] D. De Pedis,[34] P.F. Derwent,[3] C. Dionisi,[34] J.R. Dittmann,[3] A. Dominguez,[13] S. Donati,[18] M. D'Onofrio,[31] T. Dorigo,[12] N. Eddy,[29] R. Erbacher,[3] D. Errede,[29] S. Errede,[29] R. Eusebi,[25] S. Farrington,[20] R.G. Feild,[35] J.P. Fernandez,[14] C. Ferretti,[5] R.D. Field,[1] I. Fiori,[18] B. Flaugher,[3] L.R. Flores-Castillo,[26] G.W. Foster,[3] M. Franklin,[36] J. Friedman,[6] H. Frisch,[37] I. Furic,[6] M. Gallinaro,[23] M. Garcia-Sciveres,[13] A.F. Garfinkel,[14] C. Gay,[35] D.W. Gerdes,[5] E. Gerstein,[38] S. Giagu,[34] P. Giannetti,[18] K. Giolo,[14] M. Giordani,[19] P. Giromini,[17] V. Glagolev,[9] D. Glenzinski,[3] M. Gold,[39] N. Goldschmidt,[5] J. Goldstein,[11] G. Gomez,[40] M. Goncharov,[41] I. Gorelov,[39] A.T. Goshaw,[22] Y. Gotra,[26] K. Goulianos,[23] A. Gresele,[28] C. Grosso-Pilcher,[37] M. Guenther,[14] J. Guimaraes da Costa,[36] C. Haber,[13] S.R. Hahn,[3] E. Halkiadakis,[25] R. Handler,[21] F. Happacher,[17] K. Hara,[42] R.M. Harris,[3] F. Hartmann,[43] K. Hatakeyama,[23] J. Hauser,[44] J. Heinrich,[4] M. Hennecke,[43] M. Herndon,[15] C. Hill,[2] A. Hocker,[25] K.D. Hoffman,[37] S. Hou,[7] B.T. Huffman,[11] R. Hughes,[30] J. Huston,[27] C. Issever,[2] J. Incandela,[2] G. Introzzi,[18] M. Iori,[34] A. Ivanov,[25] Y. Iwata,[45] B. Iyutin,[6] E. James,[3] M. Jones,[14] T. Kamon,[41] J. Kang,[5] M. Karagoz Unel,[46] S. Kartal,[3] H. Kasha,[35] Y. Kato,[47] R.D. Kennedy,[3] R. Kephart,[3] B. Kilminster,[25] D.H. Kim,[48] H.S. Kim,[29] M.J. Kim,[38] S.B. Kim,[48] S.H. Kim,[42] T.H. Kim,[6] Y.K. Kim,[37] M. Kirby,[22] L. Kirsch,[24] S. Klimenko,[1] P. Koehn,[30] K. Kondo,[8] J. Konigsberg,[1] A. Korn,[6] A. Korytov,[1] J. Kroll,[4] M. Kruse,[22] V. Krutelyov,[41] S.E. Kuhlmann,[10] N. Kuznetsova,[3] A.T. Laasanen,[14] S. Lami,[23] S. Lammel,[3] J. Lancaster,[22] K. Lannon,[30] M. Lancaster,[49] R. Lander,[16] A. Lath,[32] G. Latino,[39] T. LeCompte,[10] Y. Le,[15] J. Lee,[25] S.W. Lee,[41] N. Leonardo,[6] S. Leone,[18] J.D. Lewis,[3] K. Li,[35] C.S. Lin,[3] M. Lindgren,[44] T.M. Liss,[29] T. Liu,[3] D.O. Litvintsev,[3] N.S. Lockyer,[4] A. Loginov,[50] M. Loreti,[12] D. Lucchesi,[12] P. Lukens,[3] L. Lyons,[11] J. Lys,[13] R. Madrak,[36] K. Maeshima,[3] P. Maksimovic,[15] L. Malferrari,[28] M. Mangano,[18] G. Manca,[11] M. Mariotti,[12] M. Martin,[15] A. Martin,[35] V. Martin,[46] M. Martínez,[3] P. Mazzanti,[28] K.S. McFarland,[25] P. McIntyre,[41] M. Menguzzato,[12] A. Menzione,[18] P. Merkel,[3] C. Mesropian,[23] A. Meyer,[3] T. Miao,[3] R. Miller,[27] J.S. Miller,[5] S. Miscetti,[17] G. Mitselmakher,[1] N. Moggi,[28] R. Moore,[3] T. Moulik,[14] M. Mulhearn,[6] A. Mukherjee,[3] T. Muller,[43] A. Munar,[4] P. Murat,[3] J. Nachtman,[3] S. Nahn,[35] I. Nakano,[45] R. Napora,[15] F. Niell,[5] C. Nelson,[3] T. Nelson,[3] C. Neu,[30] M.S. Neubauer,[6] C. Newman-Holmes,[3] T. Nigmanov,[26] L. Nodulman,[10] S.H. Oh,[22] Y.D. Oh,[48] T. Ohsugi,[45] T. Okusawa,[47] W. Orejudos,[13] C. Pagliarone,[18] F. Palmonari,[18] R. Paoletti,[18] V. Papadimitriou,[33] J. Patrick,[3] G. Pauletta,[19] M. Paulini,[38] T. Pauly,[11] C. Paus,[6] D. Pellett,[16] A. Penzo,[19] T.J. Phillips,[22] G. Piacentino,[18] J. Piedra,[40] K.T. Pitts,[29] A. Pompoš,[14] L. Pondrom,[21] G. Pope,[26] T. Pratt,[11] F. Prokoshin,[9] J. Proudfoot,[10] F. Ptohos,[17] O. Poukhov,[9] G. Punzi,[18] J. Rademacker,[11] A. Rakitine,[6] F. Ratnikov,[32] H. Ray,[5] A. Reichold,[11] P. Renton,[11] M. Rescigno,[34] F. Rimondi,[28] L. Ristori,[18] W.J. Robertson,[22] T. Rodrigo,[40] S. Rolli,[51] L. Rosenson,[6] R. Roser,[3] R. Rossin,[12] C. Rott,[14] A. Roy,[14] A. Ruiz,[40] D. Ryan,[51] A. Safonov,[16] R. St. Denis,[20] W.K. Sakumoto,[25] D. Saltzberg,[44] C. Sanchez,[30] A. Sansoni,[17] L. Santi,[19] S. Sarkar,[34] P. Savard,[52] A. Savoy-Navarro,[3] P. Schlabach,[3] E.E. Schmidt,[3] M.P. Schmidt,[35] M. Schmitt,[46] L. Scodellaro,[12] A. Scribano,[18] A. Sedov,[14] S. Seidel,[39] Y. Seiya,[42] A. Semenov,[9] F. Semeria,[28] M.D. Shapiro,[13] P.F. Shepard,[26] T. Shibayama,[42] M. Shimojima,[42] M. Shochet,[37] A. Sidoti,[12] A. Sill,[33] P. Sinervo,[52] A.J. Slaughter,[35] K. Sliwa,[51] F.D. Snider,[3] R. Snihur,[49] M. Spezziga,[33] F. Spinella,[18] M. Spiropulu,[2] L. Spiegel,[3] A. Stefanini,[18] J. Strologas,[39] D. Stuart,[2] A. Sukhanov,[1] K. Sumorok,[6] T. Suzuki,[42] R. Takashima,[45] K. Takikawa,[42] M. Tanaka,[10] M. Tecchio,[5] R.J. Tesarek,[3] P.K. Teng,[7] K. Terashi,[23]

S. Tether,[6] J. Thom,[3] A.S. Thompson,[20] E. Thomson,[30] P. Tipton,[25] S. Tkaczyk,[3] D. Toback,[41] K. Tollefson,[27] D. Tonelli,[18] M. Tönnesmann,[27] H. Toyoda,[47] W. Trischuk,[52] J. Tseng,[6] D. Tsybychev,[1] N. Turini,[18] F. Ukegawa,[42] T. Unverhau,[20] T. Vaiciulis,[25] A. Varganov,[5] E. Vataga,[18] S. Vejcik III,[3] G. Velev,[3] G. Veramendi,[13] R. Vidal,[3] I. Vila,[40] R. Vilar,[40] I. Volobouev,[13] M. von der Mey,[44] R.G. Wagner,[10] R.L. Wagner,[3] W. Wagner,[43] Z. Wan,[32] C. Wang,[22] M.J. Wang,[7] S.M. Wang,[1] B. Ward,[20] S. Waschke,[20] D. Waters,[49] T. Watts,[32] M. Weber,[13] W.C. Wester III,[3] B. Whitehouse,[51] A.B. Wicklund,[10] E. Wicklund,[3] H.H. Williams,[4] P. Wilson,[3] B.L. Winer,[30] S. Wolbers,[3] M. Wolter,[51] S. Worm,[32] X. Wu,[31] F. Würthwein,[6] U.K. Yang,[37] W. Yao,[13] G.P. Yeh,[3] K. Yi,[15] J. Yoh,[3] T. Yoshida,[47] I. Yu,[48] S. Yu,[4] J.C. Yun,[3] L. Zanello,[34] A. Zanetti,[19] F. Zetti,[13] and S. Zucchelli[13]

(CDF Collaboration)

[1]*University of Florida, Gainesville, Florida 32611*
[2]*University of California at Santa Barbara, Santa Barbara, California 93106*
[3]*Fermi National Accelerator Laboratory, Batavia, Illinois 60510*
[4]*University of Pennsylvania, Philadelphia, Pennsylvania 19104*
[5]*University of Michigan, Ann Arbor, Michigan 48109*
[6]*Massachusetts Institute of Technology, Cambridge, Massachusetts 02139*
[7]*Institute of Physics, Academia Sinica, Taipei, Taiwan 11529, Republic of China*
[8]*Waseda University, Tokyo 169, Japan*
[9]*Joint Institute for Nuclear Research, RU-141980 Dubna, Russia*
[10]*Argonne National Laboratory, Argonne, Illinois 60439*
[11]*University of Oxford, Oxford OX1 3RH, United Kingdom*
[12]*Universita di Padova, Istituto Nazionale di Fisica Nucleare, Sezione di Padova, I-35131 Padova, Italy*
[13]*Ernest Orlando Lawrence Berkeley National Laboratory, Berkeley, California 94720*
[14]*Purdue University, West Lafayette, Indiana 47907*
[15]*The Johns Hopkins University, Baltimore, Maryland 21218*
[16]*University of California at Davis, Davis, California 95616*
[17]*Laboratori Nazionali di Frascati, Istituto Nazionale di Fisica Nucleare, I-00044 Frascati, Italy*
[18]*Istituto Nazionale di Fisica Nucleare, University and Scuola Normale Superiore of Pisa, I-56100 Pisa, Italy*
[19]*Istituto Nazionale di Fisica Nucleare, University of Trieste/ Udine, Italy*
[20]*Glasgow University, Glasgow G12 8QQ, United Kingdom*
[21]*University of Wisconsin, Madison, Wisconsin 53706*
[22]*Duke University, Durham, North Carolina 27708*
[23]*Rockefeller University, New York, New York 10021*
[24]*Brandeis University, Waltham, Massachusetts 02254*
[25]*University of Rochester, Rochester, New York 14627*
[26]*University of Pittsburgh, Pittsburgh, Pennsylvania 15260*
[27]*Michigan State University, East Lansing, Michigan 48824*
[28]*Istituto Nazionale di Fisica Nucleare, University of Bologna, I-40127 Bologna, Italy*
[29]*University of Illinois, Urbana, Illinois 61801*
[30]*The Ohio State University, Columbus, Ohio 43210*
[31]*University of Geneva, CH-1211 Geneva 4, Switzerland*
[32]*Rutgers University, Piscataway, New Jersey 08855*
[33]*Texas Tech University, Lubbock, Texas 79409*
[34]*Instituto Nazionale de Fisica Nucleare, Sezione di Roma, University di Roma I, "La Sapienza," I-00185 Roma, Italy*
[35]*Yale University, New Haven, Connecticut 06520*
[36]*Harvard University, Cambridge, Massachusetts 02138*
[37]*Enrico Fermi Institute, University of Chicago, Chicago, Illinois 60637*
[38]*Carnegie Mellon University, Pittsburgh, Pennsylvania 15213*
[39]*University of New Mexico, Albuquerque, New Mexico 87131*
[40]*Instituto de Fisica de Cantabria, CSIC-University of Cantabria, 39005 Santander, Spain*
[41]*Texas A&M University, College Station, Texas 77843*
[42]*University of Tsukuba, Tsukuba, Ibaraki 305, Japan*
[43]*Institut für Experimentelle Kernphysik, Universität Karlsruhe, 76128 Karlsruhe, Germany*
[44]*University of California at Los Angeles, Los Angeles, California 90024*
[45]*Hiroshima University, Higashi-Hiroshima 724, Japan*
[46]*Northwestern University, Evanston, Illinois 60208*
[47]*Osaka City University, Osaka 588, Japan*
[48]*Center for High Energy Physics: Kyungpook National University, Taegu 702-701; Seoul National University, Seoul 151-742; and SungKyunKwan University, Suwon 440-746; Korea*
[49]*University College London, London WC1E 6BT, United Kingdom*
[50]*Institution for Theoretical and Experimental Physics, ITEP, Moscow 117259, Russia*

[51] Tufts University, Medford, Massachusetts 02155
[52] Institute of Particle Physics, University of Toronto, Toronto M5S 1A7, Canada
(Dated: June 24, 2018)

We present a new search for H^0V production, where H^0 is a scalar Higgs boson decaying into $b\bar{b}$ with branching ratio β, and V is a Z^0 boson decaying into e^+e^-, $\mu^+\mu^-$, or $\nu\bar{\nu}$. This search is then combined with previous searches for H^0V where V is a $W^\pm$ boson or a hadronically decaying Z^0. The data sample consists of 106 ± 4 pb^{-1} of $p\bar{p}$ collisions at $\sqrt{s} = 1.8$ TeV accumulated by the Collider Detector at Fermilab. Observing no evidence of a signal, we set 95% Bayesian credibility level upper limits on $\sigma(p\bar{p} \to H^0V) \times \beta$. For H^0 masses of 90, 110 and 130 GeV/c^2, the limits are 7.8, 7.2, and 6.6 pb respectively.

PACS numbers: 14.70.-e, 13.85.Qk, 13.85.Ni

A key component of the standard model (SM) is spontaneous electroweak symmetry breaking, which gives rise to the mass of all fermions and the $W^\pm$ and Z^0 gauge bosons. This process leads to the existence of a neutral scalar particle, the Higgs boson (H^0), whose mass is unspecified in the SM, but whose couplings to all other particles of known mass are fully specified at tree level. The Higgs boson has not been directly observed, but its expected contribution to loop corrections for many SM observables has allowed an inferred mass of $M_H = 126^{+73}_{-48}$ GeV/c^2 from precision electroweak measurements [1]. In addition, direct searches at LEP 2 have excluded, with a 95% confidence level, a SM Higgs boson with $M_H < 114.4$ GeV/c^2 [2]. The relatively low H^0 mass favored within the SM framework implies the possibility of its direct observation at the Tevatron in Run II, where searches have begun by both the DØ [3] and CDF collaborations. Here we report on direct searches using data accumulated by the Collider Detector at Fermilab (CDF) between February 1992 and July 1995 (Run I) for a total integrated luminosity of 106 ± 4 pb^{-1}.

At the Tevatron, the SM Higgs boson is produced from both gluon-gluon and quark-antiquark initial states [4]. Although the dominant production mechanism is $gg \to H^0$, production in association with vector bosons ($q\bar{q}' \to H^0W^\pm$, $q\bar{q} \to H^0Z^0$) provides the most sensitive channels for Higgs boson searches at the Tevatron if $M_H <$ 140 GeV/c^2, because one can obtain significant background rejection from the additional highly energetic objects in the event coming from the vector boson decays. The predicted cross section, σ_{VH^0}, for VH^0 production from $p\bar{p}$ collisions at $\sqrt{s} = 1.8$ TeV varies between 0.50 and 0.15 pb for H^0 masses between 90 and 130 GeV/c^2, with the ratio $\sigma_{W^\pm H^0}/\sigma_{Z^0H^0} \approx 1.6$.

We have previously reported the results of searches in the $WH^0 \to \ell\nu\, b\bar{b}$ ($\ell = e$ or μ) and $VH^0 \to q\bar{q}'\, b\bar{b}$ channels [5, 6]. Here we add the searches for Z^0H^0 production using the decay channels $\ell^+\ell^-\, b\bar{b}$ and $\nu\bar{\nu}\, b\bar{b}$. Finding no evidence for Higgs boson production using these decay modes, we set limits on the production cross section as a function of mass, and combine our results with the previous VH^0 cross section limits. These limits represent the final CDF cross section limits for Higgs boson production in association with a vector boson from the Run I data.

The CDF detector is described in Ref.[7], and the coordinate system and various quantities used throughout this paper are defined in Ref. [8]. The momenta of the charged leptons are measured with the central tracking chamber in a 1.4 T superconducting solenoidal magnet. Electromagnetic and hadronic calorimeters surrounding the tracking chambers are used to identify electrons and jets and measure their energies. Muons are identified with drift chambers located outside the calorimeters. The silicon vertex detector (SVX) is the innermost detector used for precise tracking in the plane transverse to the beam [9].

In the analyses reported here, two algorithms using tracks measured with the SVX are applied to identify jets originating from heavy flavor quarks (b and c). The first reconstructs a secondary vertex (a vertex displaced from the primary interaction vertex) produced by the heavy flavor decays and measures the transverse decay length (SVX tag). The resolution of the transverse decay length of the secondary vertex is typically of order 150 μm. The second algorithm uses the impact parameter of the tracks in the jet (the closest distance of the track to the primary vertex in the transverse plane) to calculate a probability that the jet is not from heavy flavor (JPB tag). The details of these tagging algorithms are given in Ref. [10].

For the details of the analyses previously published we refer to those publications [5, 6], and list the results here when appropriate, as they are used in the combined cross section limits. We now describe the two new channels, $\ell^+\ell^-\, b\bar{b}$ and $\nu\bar{\nu}\, b\bar{b}$. Events for the $\ell^+\ell^-\, b\bar{b}$ channel analysis are required to pass a high-P_T lepton trigger and must contain two high-P_T [8], oppositely charged leptons (e or μ) that are isolated from nearby tracks and calorimeter activity. At least one lepton is required to have $P_T > 20$ GeV/c and be in the central detector ($|\eta| < 1.0$). For the second lepton the P_T requirement is relaxed to 10 GeV/c and the pseudorapidity range is extended into the plug calorimeter, up to $|\eta| \sim 2.4$. The dilepton invariant mass must be in the range $76 < M_{\ell\ell} < 106$ GeV/c^2 to be consistent with the decay of a Z^0 boson. This requirement essentially removes any sensitivity of this analysis to $Z^0 \to \tau^+\tau^-$. The event is additionally required to contain two or three high-E_T jets ($E_T > 15$ GeV), at least one of which is SVX tagged. A cut on the missing transverse energy ($\not{E}_T < 50$ GeV) [8] is also applied, with the effect of reducing the $t\bar{t}$ background by approximately a factor of two, while preserving about 95% of the signal.

The $\nu\bar{\nu}\, b\bar{b}$ channel is characterized by two heavy flavor jets and large $\not{E}_T$ from the neutrinos. The data sample for this channel is derived from an event trigger requiring $\not{E}_T > 35\,\mathrm{GeV}$ in addition to event quality cuts [11]. To reject $W^{\pm}$ and Z^0 decays to leptons, events containing an isolated track with $P_T > 10\,\mathrm{GeV}/c$ are removed from the sample. To ensure less susceptibility to the uncertainty in the trigger efficiency at threshold, the analysis requires $\not{E}_T > 40\,\mathrm{GeV}$. The trigger efficiency is approximately 60% at this value of $\not{E}_T$. Additionally the event must contain two or three jets with $E_T > 15\,\mathrm{GeV}$ (about 20% of the ZH^0 signal contains a third jet). To reject QCD multi-jet events where the $\not{E}_T$ results from a mismeasured jet, the azimuthal angle between the $\not{E}_T$ and the direction of any jet with $E_T > 8\,\mathrm{GeV}$ is required to be at least 1.0 radians. In addition, the jets from inclusive di-jet production tend to be back-to-back, while jets from $H^0 \to b\bar{b}$ in ZH^0 events tend to have a smaller opening angle, leading to the requirement that the azimuthal angle between the leading two jets be less than 2.6 radians. Approximately 10% of the efficiency from the $\nu\bar{\nu}\, b\bar{b}$ selection is contributed by $W^{\pm}H^0$ events where the lepton is undetected.

Events in the $\nu\bar{\nu}\, b\bar{b}$ sample are classified as "single-tagged" (exactly one SVX tagged jet) or "double-tagged" (one SVX tagged jet and a second jet tagged by either the SVX or JPB tagging algorithms). The backgrounds and efficiencies are calculated separately for these orthogonal sets, which are then treated as separate but correlated channels when combined with the other channels. This is analogous to what was done in the $WH^0 \to \ell\nu\, b\bar{b}$ search [5].

TABLE I: Total selection efficiencies for VH^0 events in each analysis channel used in the combined result, as a function of the H^0 mass, M_H (GeV/c^2). Numbers are percentages and include the branching ratios of the vector boson ($W^{\pm}$ or Z^0) in a given channel. ST refers to single-tagged events and DT to double-tagged events. Uncertainties include systematic effects.

	VH^0 event efficiencies (%)		
Channel	$M_H = 90$	$M_H = 110$	$M_H = 130$
$\ell^+\ell^-\, bb$	0.14 ± 0.03	0.20 ± 0.04	0.19 ± 0.04
$\nu\bar{\nu}\, b\bar{b}$ (ST)	0.51 ± 0.10	0.63 ± 0.13	0.76 ± 0.15
$\nu\bar{\nu}\, b\bar{b}$ (DT)	0.37 ± 0.08	0.43 ± 0.09	0.51 ± 0.10
$\ell\nu\, b\bar{b}$ (ST)	0.59 ± 0.15	0.72 ± 0.18	0.80 ± 0.20
$\ell\nu\, b\bar{b}$ (DT)	0.22 ± 0.06	0.29 ± 0.07	0.30 ± 0.08
$q\bar{q}'\, b\bar{b}$	1.3 ± 0.7	2.2 ± 1.1	3.1 ± 1.6

The efficiencies for identifying VH^0 events with our selection criteria are summarized in Table I and are determined from a PYTHIA [12] Monte Carlo simulation of Higgs boson production via $V^* \to VH^0 \to Vb\bar{b}$ followed by a detector simulation. The Higgs boson is forced to decay to $b\bar{b}$ with a 100% branching ratio. The identification efficiencies for single leptons are measured from $Z^0 \to \ell^+\ell^-$ events in the data and are found to be 91% for muons and 83% for electrons [13]. The SVX and JPB b-tagging efficiencies are determined using data and Monte Carlo samples with high b-purity [10]. In the $\ell^+\ell^-\, b\bar{b}$ channel, the efficiency for obtaining ≥ 1 SVX tag in a signal event is (45 ± 7)%. The double b-tagging efficiency in the $\nu\bar{\nu}\, b\bar{b}$ channel (SVX + SVX or SVX + JPB) is (19 ± 4)%, and the single b-tagging efficiency (one SVX tag) is (25 ± 3)%. The total event efficiencies are the product of the trigger efficiencies, the kinematic and geometric acceptances from the selection cuts, the lepton identification efficiencies when appropriate, the b-tagging efficiencies, and the V branching ratio relevant for a given search channel. The systematic uncertainties in the total efficiencies for the $\ell^+\ell^-\, b\bar{b}$ and $\nu\bar{\nu}\, b\bar{b}$ channels are approximately 20%, comprised mostly of the uncertainties in the b-tagging efficiency (15%), the modeling of initial and final state radiation (7%), lepton identification efficiency (7% for the $\ell^+\ell^-\, b\bar{b}$ channel), trigger efficiency (5% for the $\nu\bar{\nu}\, b\bar{b}$ channel), integrated luminosity (4%) and the energy scale of jets (3%).

In the $\ell^+\ell^- b\bar{b}$ channel the dominant background is Z^0 production in association with a heavy flavor pair ($Z^0b\bar{b}$, $Z^0c\bar{c}$), which accounts for approximately 60% of the total. About 20% comes from Z^0+jets events where a jet is mistagged due to track mismeasurements, and there are smaller contributions from Z^0c, Z^0b, diboson, and $t\bar{t}$. All backgrounds are determined using Monte Carlo simulations except that from Z^0+jets which uses the data.

The $\nu\nu b\bar{b}$ channel background is dominated by QCD jet production of $b\bar{b}$ where the $\not{E}_T$ results from mismeasured jets. To calculate this contribution we first parameterize the tagging rate in the $\not{E}_T < 40$ GeV region of the data as a function of jet E_T and track multiplicity. By applying this parametrization to the jets in the signal region we estimate the QCD background to be about 70% of the total background in the single-tagged sample and about 50% in the double-tagged sample. Smaller backgrounds include $V+$ heavy flavor, diboson, and $t\bar{t}$, all of which are derived from Monte Carlo simulations.

For each decay channel, Table II summarizes the total expected backgrounds, the expectations from standard model VH^0 production for $M_H = 110$ GeV/c^2 and $H^0 \to b\bar{b}$, and the number of data events observed. The dominant background in the $q\bar{q}'b\bar{b}$ channel is QCD production of $b\bar{b}$ with additional jets, hereafter abbreviated as "QCD". Its normalization is difficult to predict and therefore left unconstrained in the analysis. Further details of the background calculations are given elsewhere [5, 6, 10].

TABLE II: Predicted numbers of events in each channel from all backgrounds (see text), expected number of signal events for $M_H = 110$ GeV/c^2, and number of events observed. Uncertainties include systematic effects. There is no reliable prediction for the background in the $q\bar{q}'\,b\bar{b}$ channel.

Channel	Background	Signal	Data
$\ell^+\ell^-\,bb$	3.2 ± 0.7	0.06 ± 0.01	5
$\nu\bar{\nu}\,b\bar{b}$ (ST)	39 ± 4	0.20 ± 0.04	40
$\nu\bar{\nu}\,b\bar{b}$ (DT)	3.9 ± 0.6	0.14 ± 0.03	4
$\ell\nu\,b\bar{b}$ (ST)	30 ± 5	0.23 ± 0.06	36
$\ell\nu\,b\bar{b}$ (DT)	3.0 ± 0.6	0.09 ± 0.02	6
$q\bar{q}'\,b\bar{b}$		0.73 ± 0.29	589

A binned likelihood is used to compare the dijet mass spectrum (of the two tagged jets, or the one tagged jet and highest-E_T untagged jet) in the data to a combination of expected distributions from the background processes and the VH^0 signal, as a function of H^0 mass. The observed dijet mass spectra for the $\nu\bar{\nu}\,b\bar{b}$ and $\ell^+\ell^-\,b\bar{b}$ channels are shown together with the expected background shapes in Figs. 1 and 2 respectively.

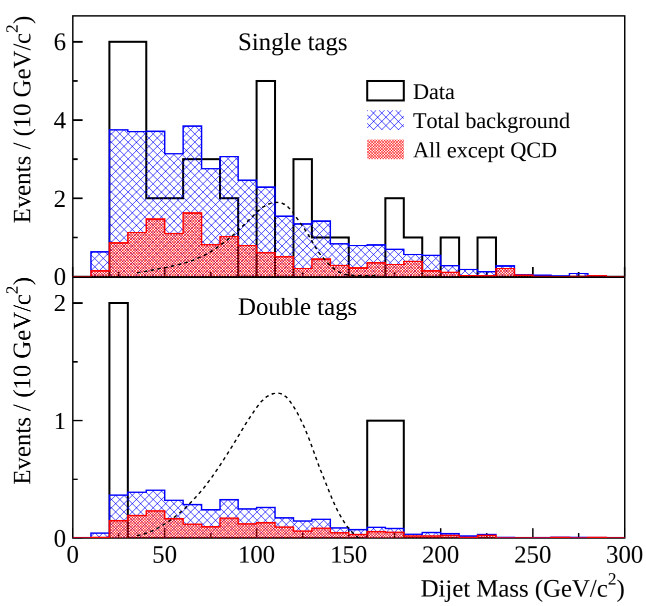

FIG. 1: Dijet invariant mass in $\nu\bar{\nu}\,b\bar{b}$ candidate events, for events with exactly one b-tagged jet and separately for events with two b-tagged jets. The single b-tag data includes one overflow event. The background shapes shown differ only in the inclusion of the predominant background of QCD $b\bar{b}$ production. The signal shape shown (dashed line) is for a SM Higgs mass of 110 GeV/c^2 and a normalization of 50 times the expected rate.

Since no signal is observed, we calculate upper limits on VH^0 production using a Bayesian procedure. For each channel, a posterior density is obtained by multiplying the likelihood function for that channel with prior densities for all the parameters in the likelihood: integrated luminosity, background normalizations, signal efficiency, and the product $\sigma'_{VH^0} \equiv \sigma_{VH^0} \times \beta$ of the signal cross section σ_{VH^0} by the branching ratio β for $H^0 \to b\bar{b}$. With two exceptions, these priors are truncated Gaussian densities constraining a given parameter to its expected value within its uncertainty. The exceptions are σ'_{VH^0} and the QCD background normalization in the $q\bar{q}'\,b\bar{b}$ channel. Since nothing is presumed known a priori about these parameters, they are assigned uniform priors. The posterior density is then integrated over all parameters except σ'_{VH^0}, and a 95% credibility level (C.L.) upper limit on σ'_{VH^0} is obtained by calculating the 95$^{\rm th}$ percentile of the resulting distribution. When combining channels, the same procedure is applied to the product of their likelihoods. Correlations in the total efficiencies are taken into account by identifying common parameters such as the b-tagging efficiency and some kinematical efficiencies. Each of these common parameters is then assigned a single prior.

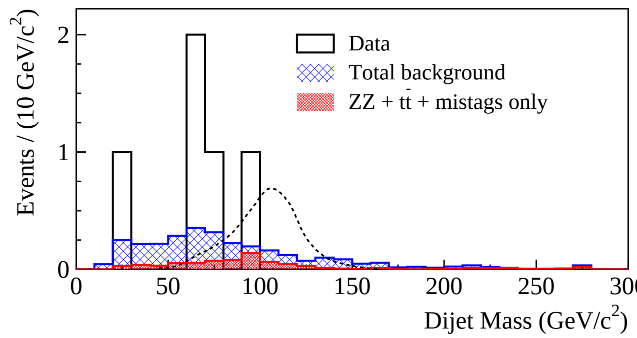

FIG. 2: Dijet invariant mass in $\ell^+\ell^-\,b\bar{b}$ candidate events. At least one jet is required to be b-tagged by the SVX algorithm. The background shapes shown differ only in the inclusion of the predominant background of Z^0+heavy flavor. The signal shape shown (dashed line) is for a SM Higgs mass of 110 GeV/c^2 and a normalization of 50 times the expected rate.

Upper limits on $\sigma_{VH^0} \times \beta$ in each channel and in all channels combined are summarized in Table III as a function of H^0 mass.

These results are also plotted in Figure 3. The standard model prediction is about 30 times smaller than the measured 95% C.L. upper limits. For the $\ell\nu\,b\bar{b}$ and $q\bar{q}'\,b\bar{b}$ channels, the limits reported here are slightly different from those previously published [5, 6]; this is mainly due to our improved understanding of the b-tagging efficiency [10]. Table III also shows expected upper limits under the assumption of zero signal. These expectations are calculated over an ensemble of experiments similar to this one, but where the background normalizations are fluctuated around their expected values by their uncertainties. We note that the observed combined limits are driven by the

TABLE III: The 95% credibility level upper limits on $\sigma(p\bar{p} \to VH^0) \times \beta$ where $\beta = \mathrm{BR}(H^0 \to b\bar{b})$, for each of the search channels and their combination, as a function of H^0 mass, M_H (GeV/c^2). Also shown are the expected limits under the assumption of no H^0 signal. ST designates the single b-tagged subsample and DT the double b-tagged subsample.

Channel	Measured (expected) upper limits (pb) $M_H = 90$	$M_H = 110$	$M_H = 130$
$\ell^+\ell^-\, bb$	55.6 (36)	31.8 (24)	23.8 (25)
$\nu\bar{\nu}\, b\bar{b}$ (ST)	20.8 (30)	20.8 (21)	18.4 (17)
$\nu\bar{\nu}\, b\bar{b}$ (DT)	10.4 (17)	9.2 (14)	8.0 (12)
$\nu\bar{\nu}\, b\bar{b}$ (ST+DT)	7.6 (13)	7.8 (11)	7.4 (8.8)
$\ell\nu\, b\bar{b}$ (ST)	30.0 (18)	29.4 (15)	27.6 (12)
$\ell\nu\, b\bar{b}$ (DT)	31.0 (24)	26.6 (19)	24.2 (18)
$\ell\nu\, b\bar{b}$ (ST+DT)	23.2 (13)	22.6 (11)	21.6 (9.0)
$q\bar{q}'\, b\bar{b}$	38.2 (77)	21.2 (43)	17.8 (29)
All combined	7.8 (7.1)	7.2 (5.7)	6.6 (4.7)

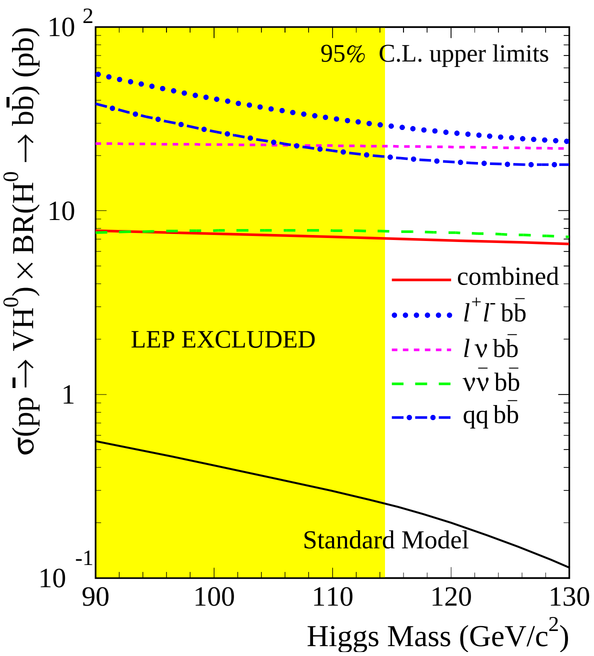

FIG. 3: Summary of all Run I CDF 95% credibility level upper limits on $\sigma(p\bar{p} \to VH^0) \cdot \beta$. The lines for the $\nu\bar{\nu}\, b\bar{b}$ and $\ell\nu\, b\bar{b}$ channels represent the combined limits from the single b-tagged and double b-tagged subsamples. Shown for comparison is the standard model prediction, and the region excluded by the LEP experiments.

$\nu\bar{\nu}\, b\bar{b}$ channel, as a result of an observed downward fluctuation in the dijet invariant mass region of interest in this channel. However, the expectation is for the $\nu\bar{\nu}\, b\bar{b}$ and $\ell\nu\, b\bar{b}$ channels to have comparable sensitivity.

In conclusion, we have searched for Z^0H^0 production using the $\ell^+\ell^-$ and $\nu\bar{\nu}$ decay channels of the Z^0 and produced limits on VH^0 production using these channels. We combined these limits with those previously published using other decay channels of the vector bosons to obtain final CDF Run I 95% C.L. limits on $\sigma_{VH^0} \times \beta$ ranging from 7.8 pb to 6.6 pb for H^0 masses of 90 GeV/c^2 to 130 GeV/c^2. These limits additionally apply to any scalar particle decaying to $b\bar{b}$ that is produced in association with a vector boson. These results and the combination methodology establish the foundation for our searches in the Tevatron Run II data at $\sqrt{s} = 1.96$ TeV which are exploiting more search channels, an improved detector, and more advanced analysis techniques [14].

We thank the Fermilab staff and the technical staffs of the participating institutions for their contributions. This work was supported by the U.S. Department of Energy and National Science Foundation; the Italian Istituto Nazionale di Fisica Nucleare; the Ministry of Science, Culture, and Education of Japan; the Natural Sciences and Engineering Research Council of Canada; the National Science Council of the Republic of China; and the A. P. Sloan Foundation.

[1] The LEP Electroweak Working Group, `http://lepewwg.web.cern.ch/LEPEWWG/`; V.M. Abazov *et al.*, Nature **429**, 638 (2004).
[2] R. Barate *et al.*, Phys. Lett. B **565**, 61 (2003).
[3] V.M. Abazov *et al.*, hep-ex/0410062, submitted to Phys. Rev. Lett..
[4] A. Stange, W. Marciano and S. Willenbrock, Phys. Rev. D**49**, 1354 (1994).
[5] F. Abe *et al.*, Phys. Rev. Lett. **79**, 3819 (1997).
[6] F. Abe *et al.*, Phys. Rev. Lett. **81**, 5748 (1998).
[7] F. Abe *et al.*, Nucl. Instr. Meth. Phys. Res. A **271**, 387 (1988).
[8] In the CDF coordinate system, θ and ϕ are the polar and azimuthal angles, respectively, with respect to the proton beam direction (z axis). The pseudorapidity η is defined as $-\ln\tan(\theta/2)$. The transverse momentum of a particle is $P_T = P\sin\theta$. The analogous quantity using calorimeter energies, defined as $E_T = E\sin\theta$, is called transverse energy. The missing transverse energy, $\not{E}_T$, is defined as $-\sum E_T^i\,\hat{n}_i$, where $\hat{n}_i$ is the unit vector in the transverse plane pointing from the interaction point to the energy deposition in calorimeter cell i.
[9] D. Amidei *et al.*, Nucl. Instr. Meth. Phys. Res. A **350**, 73 (1994).
[10] T. Affolder *et al.*, Phys. Rev. D**64**, 032002 (2001).
[11] T. Affolder *et al.*, Phys. Rev. Lett. **88**, 041801 (2002).
[12] T. Sjöstrand, Comput. Phys. Commun. **82**, 74 (1994). We use PYTHIA V5.7.
[13] F. Abe *et al.*, Phys. Rev. Lett. **80**, 2779 (1998).
[14] L. Babukhadia *et al.* (CDF and DØ Higgs Sensitivity Working Group), FERMILAB-PUB-03-320-E (2003); C. Neu (CDF collaboration), FERMILAB-CONF-04-027-E (2004).